Magmatic Densities Control Erupted Volumes in Icelandic Volcanic Systems

Margaret Hartley [1,2,*] **and John Maclennan** [2]

[1] *School of Earth and Environmental Sciences, University of Manchester, UK*
[2] *Department of Earth Sciences, University of Cambridge, UK*

Correspondence*:
Margaret Hartley, School of Earth and Environmental Sciences, University of Manchester, Williamson Building, Oxford Road, Manchester, M13 9PL, UK
margaret.hartley@manchester.ac.uk

ABSTRACT

The control of magmatic physical properties on the range and volumetric distribution of eruptions has been investigated for the active volcanic zones of Iceland. Magmatic density and viscosity both exert control over observed erupted volumes. The largest volume of erupted material sits at a density and viscosity minimum corresponding to the composition of basalts at the arrival of plagioclase on the liquidus. These basalts are buoyant with respect to the upper crust. Almost 70% of the erupted volume in Iceland's Northern Volcanic Zone (NVZ) comprises basalts that lie close to this minimum. However, small volume eruptions with densities greater than those of the upper crust are found in Iceland. Amongst these eruptions are the picrites, and it is likely that their eruption is facilitated by the generation of overpressure in magma chambers in the lower crust and uppermost mantle. This conclusion is in agreement with petrological constraints on the depth of crystallisation under Iceland.

Keywords: Magma, Basalt, Iceland, Density, Viscosity, Volcanism, Volumes

1 INTRODUCTION

It has long been understood that the range of lava compositions sampled at mid-ocean ridges is strongly linked to the buoyancy of melt in the oceanic crust (*Huppert and Sparks*, 1980; *Sparks et al.*, 1980) and the viscosity of the melt (*Walker*, 1971). Magmas generated at depth are expected to rise through the crust until ρ_m-ρ_c $\approx$0, that is, the point at which the magma density ρ_m and crustal density ρ_c are equal. The ponding of magmas at their level of neutral buoyancy in the crust (*Ryan*, 1993) is considered to be an important factor in the prolonged existence of sub-caldera magma chambers (*Ryan*, 1987b).

Neutral buoyancy concepts can also be applied within magma chambers. *Huppert and Sparks* (1980) and *Sparks et al.* (1980) consider a fluid-dynamical approach within layered magma chambers to explore the conditions under which magma is erupted at the surface. As melt crystallises within the chamber, the density of the residual liquid evolves until a density minimum is reached. Typical suites of mid-ocean ridge basalts (MORB) reach this density minimum at $\sim$7-10 wt.% MgO (*Sparks and Huppert*, 1984). These residual liquids may then ascend to their level of neutral buoyancy, leaving the magma chamber by means of eruption. *Stolper and Walker* (1980) define a 'window of eruptibility' for potential eruptive magmas, with the crust acting as a density filter to high-MgO magmas. This window is found at magnesium numbers (Mg#, molar Mg/(Mg+Fe^{2+}) of 0.55-0.75. The fluid-dynamical approach thus predicts that high-MgO eruptions will not occur (*Huppert and Sparks*, 1980). However, picritic eruptions with $>$15 wt.% MgO and whole-rock Mg#$>$0.8 have been recorded in Iceland, which cannot be explained by neutral buoyancy or fluid-dynamical approaches.

2 MAGMATISM IN ICELAND

Iceland is situated where a mantle plume underlies the Mid-Atlantic Ridge. High mantle potential temperatures within the plume cause a greater degree of melting under Iceland than under normal mid-ocean ridges, producing anomalously thick crust that is exposed above sea level. Iceland is thus the only part of the global spreading system where lava compositions can be routinely tied to eruptions of known age and volume. Iceland's active volcanic zones therefore provide an excellent opportunity to better understand the role of the crust as a density filter for magma. Previous studies of this density filter have focused on MORB compositons; however, this approach is limited since the association of samples from submerged spreading centres with individual eruptions of known age and volume has rarely been possible. The geological controls available on Iceland allow the study not only of the range of erupted compositions but also of the volumetric distribution of lavas with different compositions and different physical properties.

Neutral buoyancy and fluid-dynamical models assume that melt ascending from depth will always encounter a sub-caldera magma chamber and therefore melt ascent will always be limited to its level of neutral buoyancy. Eruption at the surface is then facilitated by crystallisation in a shallow magma chamber until the density minimum is reached. These models are appropriate for some volcanic settings in Iceland, notably central volcanoes such as Krafla where seismic surveys indicate the presence of a shallow magma chamber at $\sim$3 km depth (*Brandsdóttir et al.*, 1997). However, evidence from ophiolite sections (*Kelemen et al.*, 1997; *Korenaga and Kelemen*, 1997) and from clinopyroxene crystallisation pressures in basaltic lavas across Iceland (e.g. *Maclennan et al.*, 2001) indicate that polybaric fractional crystallisation occurs in sill-like magma reservoirs at a range of depths in the crust, including near-Moho depths of 25-30 km (0.8-1.1 GPa; *Maclennan et al.* (2003); *Maclennan* (2008); *Winpenny and Maclennan* (2011); *Neave and Putirka* (2017)). The presence of gabbroic sills in the Moho transition zone of the Semail ophiolite indicate that such magma chambers may form at depths greater than their level of magmatic neutral buoyancy (*Kelemen et al.*, 1997). Similarly, the vent positions of Iceland's lava shields are unrelated to the present-day fissure swarms and central volcanoes, and the presence of chrome-diopside in many lava shields suggests that these magmas did not undergo significant low-pressure fractionation, but were fed directly by primitive melts sourced from the base of the crust (*Sigurðsson and Sparks*, 1978). The lava shields include large-volume eruptions of more evolved basalts (e.g. Stóravíti, $\sim$30 km^3; Skjaldbreiður, $\sim$11 km^3) and smaller volumes of dense picrite containing up to 20% olivine phenocrysts (e.g. Háleyjabunga, 0.013 km^3).

3 MAGMA DENSITY AND VISCOSITY

A large dataset comprising samples from the Krafla and Theistareykir volcanic systems of Iceland's Northern Volcanic Zone (NVZ) was used to investigate the links between the physical properties of magma and the volumetric distribution of lava as a function of its composition. The samples correspond to postglacial eruptions of known volume and major element chemistry (*Slater*, 1996; *Nicholson*, 1990).

The modal proportions of olivine, plagioclase and rare clinopyroxene phenocrysts in selected samples were obtained by point counting. Phenocryst compositions were determined using a Cameca SX100 electron microprobe at the University of Cambridge, using a beam diameter of 2 μm, current of 10 nA and accelerating voltage of 15 kV for all analyses.

The density of a melt consisting of N components with mole fractions x_j (j=1,2,3...N) is typically calculated:

$$\rho = \frac{\sum_{j=1}^{N} x_j M_j}{\sum_{j=1}^{N} x_j V_j} \tag{1}$$

where M is the molar mass and V the partial molar volume. This is appropriate for calculating a whole-rock density if the sample is representative of a magmatic liquid. However, for samples with abundant accumulated phenocrysts, the whole-rock density is not representative of a magmatic liquid and its density is better calculated as follows:

$$\rho_m = F_{ol}\rho_{ol} + F_{pl}\rho_{pl} + (1 - F_{ol} - F_{pl})\rho_l \tag{2}$$

where F is a volume fraction, ρ is a density, and the subscripts ol, pl, l and m refer to olivine, plagioclase, liquid and magma (i.e. liquid plus phenocrysts) respectively. Other phenocryst phases such as clinopyroxene may also be included in this calculation; however, clinopyroxene was absent as a phenocryst phase from most of the samples considered in this study.

Point-counting data were used to correct whole-rock compositions for the presence of accumulated phenocrysts in order to obtain an estimate of the carrier liquid composition. The density and viscosity of these liquids were calculated at their liquidus temperatures with Petrolog3 (*Danyushevsky and Plechov*, 2011), using the methods of *Lange and Carmichael* (1990) and *Bottinga and Weill* (1972) respectively. The densities of phenocryst phases were calculated from their major element compositions, modelling forsterite-fayalite and albite-anorthite as ideal solid solutions with linear relationships between the densities of their endmembers (*Fei*, 1995).

Of the 89 samples examined, over half contained $<$5% accumulated phenocrysts, and the density correction associated with accumulation for these samples is negligible (2 kg m^{-3} mean). However, Theistareykir picrites contain up to 20 vol.% accumulated olivine and the magmatic densities for 12 samples containing $>$10% phenocrysts are on average 50 kg m^{-3} higher than the densities calculated under the assumption that the whole-rock composition was equivalent to an erupted liquid. The effect of errors in modal proportions from point counting on the calculated magma densities is $<$10 kg m^{-3} (*Neilson and Brockman*, 1977).

Magmatic viscosities were calculated from the liquid viscosity and accumulated phenocryst content using the Einstein-Roscoe equation:

$$\mu = \mu_0(1 - \Phi/\Phi_m)^{-n} \tag{3}$$

where μ_0 is the viscosity of the homogeneous melt and Φ is the crystal fraction. Φ_m and n are adjustable parameters that vary with the size, shape and distribution of particles in the melt; for magmatic processes these can be modelled using Marsh's constants $\Phi_m = 0.6$ and $n = 2.5$ (*Lejeune and Richet*, 1995). This method of calculating magma viscosity is appropriate for the relatively low crystal contents (Φ <30%) of the NVZ magmas; for crystal contents 30< Φ <80% a more complex viscosity model (e.g. *Costa et al.*, 2009) may be required.

At atmospheric pressure, the calculated magmatic densities show a minimum for samples with 0.635<Mg#<0.670. The density minimum roughly corresponds to the predicted arrival of plagioclase on the liquidus and the observed shift from dominantly olivine-phyric to plagioclase-phyric samples. The position of the density minimum is unaffected by the choice of pressure of calculation of the liquidus temperature. While melt densities on the liquidus of a given sample increase by $\sim$60 kg m^{-3} on increasing pressure from 0.001 to 0.9 GPa, this effect is almost uniform for all of the samples considered. Therefore, in order to highlight the control on physical properties from melt composition and accumulated phenocrysts, the results presented hereafter refer to density calculated at atmospheric pressure.

4 VOLUME CONTROL BY PHYSICAL PROPERTIES

The physical properties of magmas exert a strong control on the erupted volumes. Despite the large range in predicted densities (2695-2840 kg m^{-3}) and viscosities (2-900 Pa s) in the NVZ the largest eruptions cluster close to the density and viscosity minima (Fig. 1a). For example, 70% of the total erupted volume lies at densities <2720 kg m^{-3} and viscosities <100 Pa s. This includes samples from the postglacial lava shield Stóravíti (30 km^3), which dominates the postglacial volumetric output of the Theistareykir volcanic system. Enhanced melt production and eruption rates during early postglacial times due to deglaciation (*Jull and McKenzie*, 1996; *Maclennan et al.*, 2002) are not sufficient to explain the volume of Stóravíti, since this enhanced mantle melt production rate is common to all the early postglacial eruptions in this study. Instead, the physical properties of the Stóravíti magma are the cause of the large volume of this eruption in comparison with other early postglacial eruptions such as the Theistareykir picrites.

Only 2% of the erupted volume has predicted density >2720 kg m^{-3} and viscosity >100 Pa s. The remainder of the volume is either erupted as high viscosity, low density (20%) or low viscosity, high density (8%) magma. The volume maximum sits close to the minimum density and viscosity of magma available in the NVZ. This demonstrates the fundamental the control of density and viscosity on volumetric output.

Basalts from the NVZ typically contain 0.1-0.5 wt.% H_2O (*Nichols et al.*, 2002). The effect of adding up to 1.0 wt.% H_2O on magma density and viscosity was calculated using the methods of *Ochs and Lange* (1999) and *Whittington et al.* (2000) respectively (Fig. 1a). By varying the H_2O content of the liquid, the magma density minimum is reduced from 2700 kg m^{-3} at 0 wt.% H_2O to 2695 kg m^{-3} at 0.2 wt.% H_2O, 2690 kg m^{-3} at 0.5 wt.% H_2O and 2681 kg m^{-3} at 1.0 wt.% H_2O.

5 CRYSTALLISATION AND ACCUMULATION

The compositional array of magmas reflects the control of magmatic evolution by fractional crystallisation and melt mixing. The minimum available density and viscosity of magma is controlled by the fractionation and mixing paths of those magmas. The variation of density and viscosity as a function of melt fraction crystallised was calculated using Petrolog3. Calculations were run at a range of crustal pressures (0.001-0.9 GPa) and putative primary melt compositions. The observed maximum volumes correspond to a cusp on the predicted evolution of density and viscosity during fractional crystallisation (Fig. 1b). This cusp relates to the arrival of plagioclase on the basalt liquidus.

While upper crustal density plays an important role in controlling eruptive volumes, the eruption of dense picrites (>2800 kg m^{-3}) indicates that magma is able to rise above its level of neutral buoyancy in the crust. The eruption of such magmas is driven by the development of sufficient overpressure in near-Moho magma chambers. One way to generate this overpressure is as buoyant melts encounter local permeability barriers. The rapid crystallisation of basaltic melt lenses creates a zone of reduced porosity and permeability such that ascending melts are trapped beneath these zones. Continuous melt influx to the region beneath such a barrier leads to increasing overpressures, eventually resulting in a melt-filled fracture which may reach the surface and result in eruption, or may be halted by either encountering another permeability barrier or by reaching its level of neutral buoyancy in the crust. *Kelemen and Aharonov* (1998) develop this model based on field evidence from the Moho transition zone of the Semail ophiolite, where gabbroic sills, relics of basaltic melt lenses, formed in denser harzburgitic country rock.

6 LINKING ERUPTED VOLUMES TO PHYSICAL PROPERTIES

6.1 Constant Overpressure in a Magma Chamber

The observed relationship between density, viscosity and erupted volume can be explored using simple models of the development of overpressure in melt lenses, which relate magma viscosity, density and input flux to ascent rate, volumetric output rate and eruption frequency (*Kelemen and Aharonov*, 1998). Melt influx to melt lenses at depth h may cause a fracture of width a to form when the overpressure exceeds the fracture stress of the country rock (Fig. 3; see Table 1 for the notation used in the modelling). It is assumed that such fractures open instantaneously. Once open, the surrounding country rock is assumed to behave elastically with respect to the fracture. Melt flow through the fracture is assumed to be laminar and constant with height, and thus can be described by an average melt velocity. Assuming constant overpressure and ignoring horizontal extensional stresses, the dyke width and melt flow speed are given by:

$$a = \frac{hP_f}{G}, \qquad \omega \approx \frac{a^2}{12\mu h}(P_f + \Delta\rho g h) \tag{4}$$

The predicted flux, the product $a\omega$, was calculated using the above equations for a range of magma densities and viscosities, with P_f=1 MPa, G=10 GPa and h=10 km (Fig. 2). This generalised model is cannot encapsulate all the details of individual eruptions (for example, the assumption of constant a is unlikely to be correct) but illustrates possible mechanisms for the control exerted by physical properties. Given its simplicity, it provides a surprisingly good fit to the observed relationship between physical properties and erupted volumes. The influence of viscosity on the erupted volumes can be isolated when the magma density is held fixed in the models, or the observations filtered to lie within a narrow density range. Both model predictions are predominantly concave-up on Fig. 4a, indicating that greater erupted volumes are found at lower viscosity. The role of buoyancy is clear from inspection of the results of calculations performed with fixed magma viscosity and varying density (Fig. 4b). These model predictions indicate that as a result of the magmatic overpressure $\sim$15% of the erupted melt may have a density greater than that of the country rock. This proportion is roughly in agreement with the observations if the country rock density is assumed to be 2710 kg m^{-3}. The model results show that magma with a density $>$10 kg m^{-3} greater than that of the country rock are not erupted. However, 5-10% of the observed erupted volume is composed of magma with densities of 2730 kg m^{-3} or greater and some picrites have densities of $>$2800 kg m^{-3}, well in excess of expected Icelandic upper crustal densities. The eruption of such magma is not predicted by the simple sill models and may indicate that magma chambers feed eruptions from a variety of physical surroundings, as explored below.

6.2 Constant Volumetric Influx Rate to Magma Chamber

In order to account for the eruption of picrites through low density upper crust, the physical conditions of the magma chambers supplying Icelandic eruptions must vary. More complex models were used to investigate the role of varying magma chamber depth, country rock density and fracture strength. This fuller realisation of the models was explored by solving the differential equations for inflation of a magma chamber, fracture of its walls, release of magmatic overpressure and solidification of the dyke. Rather than maintaining constant magmatic overpressure, this scheme involves constant volumetric influx rate to the magma chamber and allows significant overpressure fluctuations to occur. The governing equations, posed by *Kelemen and Aharonov* (1998), were solved with a 4^{th} order Runge-Kutta scheme paying particular attention numerical accuracy at the time of fracture development, when predicted magma fluxes vary rapidly. The output magmatic flux was compared with an input at constant rate to the chamber.

Increasing h, decreasing P_f, or increasing G encourage eruption at high densities and viscosities (Fig. 4). Therefore, increased chamber depth may allow picrites to erupt at the surface, past their level of neutral buoyancy. Similarly, if the density of the country rock is increased, then eruption of denser magma is permitted. Magma chambers for picrites are therefore likely to be in the lower crust or uppermost mantle, where densities of $\geq$2950 kg m^{-3} are expected (*Staples et al.*, 1997). This inference is in agreement with petrological constraints on the depth of magma chambers, which indicate that crystallisation of picrites and high-Mg# basalts under Theistareykir occurs at depths of 15-30 km (*Maclennan et al.*, 2001, 2003; *Winpenny and Maclennan*, 2011).

7 CONCLUSIONS

The physical properties of magmas exert key controls on the erupted volumes from Iceland's active rift zones. The largest volume of erupted material sits at a well-defined density and viscosity minimum coincident with the arrival of plagioclase on the basalt liquidus. These basalts are buoyant with respect to the Icelandic upper crust. Almost 70% of the erupted volume in the NVZ comprises basalts that sit close to this minimum.

The density filter is, however, leaky. Several small-volume eruptions with densities greater than the Icelandic upper crust are found in the NVZ. These eruptions include the picrites, which often contain large proportions of accumulated olivine phenocrysts. It is likely that the eruption of such magmas is facilitated by the generation of overpressure in magma chambers in the lower crust or uppermost mantle. This conclusion is consistent with the petrological constraints on the depth of crystallisation of high Mg# melts under Iceland.

ACKNOWLEDGMENTS

We thank Thierry Menand and Oli Shorttle for their comments on an early version of this manuscript.

REFERENCES

Bottinga, Y., and D. F. Weill, Viscosity of magmatic silicate liquids - Model for calculation, *American Journal of Science*, *272*(5), 438–475, 1972.

Brandsdóttir, B., W. Menke, P. Einarsson, R. S. White, and R. K. Staples, Faroe-Iceland Ridge Experiment. 2. Crustal structure of the Krafla central volcano, *Journal of Geophysical Research-Solid Earth*, *102*(B4), 7867–7886, 1997.

Costa, A., L. Caricchi, and N. Bagdassarov, A model for the rheology of particle-bearing suspensions and partially molten rocks, *Geochemistry, Geophysics, Geosystems*, *10*(3), Q03,010, doi:10.1029/2008GC002138, 2009.

Danyushevsky, L. V., and P. Plechov, Petrolog3: Integrated software for modeling crystallization processes, *Geochemistry Geophysics Geosystems*, *12*(7), 1–32, doi:10.1029/2011GC003516, 2011.

Fei, Y., Thermal expansion, in *Mineral Physics and Crystallography: A Handbook of Physical Constants*, vol. 2, edited by T. J. Ahrens, pp. 29–44, AGU, Washington, D.C., 1995.

Huppert, H. E., and R. S. J. Sparks, Restrictions on the compositions of mid-ocean ridge basalts - A fluid dynamical investigation, *Nature*, *286*(5768), 46–48, 1980.

Jull, M., and D. McKenzie, The effect of deglaciation on mantle melting beneath Iceland, *Journal of Geophysical Research-Solid Earth*, *101*(B10), 21,815–21,828, 1996.

Kelemen, P. B., and E. Aharonov, Periodic formation of magma fractures and generation of layered gabbros in the lower crust beneath oceanic spreading ridges, in *Geophysical Monograph*, vol. 106, edited by W. R. Buck, P. T. Delaney, J. A. Karson, and Y. Lagabrielle, pp. 267–289, AGU, Washington, D.C., 1998.

Kelemen, P. B., K. Koga, and N. Shimizu, Geochemistry of gabbro sills in the crust-mantle transition zone of the Oman ophiolite: implications for the origin of the oceanic lower crust, *Earth and Planetary Science Letters*, *146*(3), 475–488, 1997.

Korenaga, J., and P. B. Kelemen, Origin of gabbro sills in the Moho transition zone of the Oman ophiolite: Implications for magma transport in the oceanic lower crust, *Journal of Geophysical Research*, *102*(B12), 27,729–27, 1997.

Lange, R. L., and I. S. E. Carmichael, Thermodynamic properties of silicate liquids with emphasis on density, thermal-expansion and compressibility, *Reviews in Mineralogy and Geochemistry*, *24*, 25–64, 1990.

Lejeune, A. M., and P. Richet, Rheology of crystal-bearing silicate melts - an experimental study at high viscosities, *Journal of Geophysical Research-Solid Earth*, *100*(B3), 4215–4229, 1995.

Maclennan, J., Concurrent mixing and cooling of melts under Iceland, *Journal of Petrology*, *49*, 1931–1953, 2008.

Maclennan, J., D. McKenzie, K. Grönvold, and L. Slater, Crustal accretion under northern Iceland, *Earth and Planetary Science Letters*, *191*(3-4), 295–310, 2001.

Maclennan, J., M. Jull, D. McKenzie, L. Slater, and K. Grönvold, The link between volcanism and deglaciation in Iceland, *Geochemistry Geophysics Geosystems*, *3*, doi:10.1029/2001GC000282, 1062, 2002.

Maclennan, J., D. McKenzie, K. Grönvold, N. Shimizu, J. M. Eiler, and N. Kitchen, Melt mixing and crystallization under Theistareykir, northeast Iceland, *Geochemistry Geophysics Geosystems*, *4*, doi:10.1029/2003GC000558, 8624, 2003.

Neave, D. A., and K. D. Putirka, A new clinopyroxene-liquid barometer, and implications for magma storage pressures under Icelandic rift zones, *American Mineralogist*, *102*(4), 777–794, 2017.

Neilson, M. J., and G. F. Brockman, The error associated with point-counting, *American Mineralogist*, *62*(11-12), 1238–1244, 1977.

Nichols, A. R. L., M. R. Carroll, and A. Hóskuldsson, Is the Iceland hot spot also wet? Evidence from the water contents of undegassed submarine and subglacial pillow basalts, *Earth and Planetary Science Letters*, *202*, 77–87, 2002.

Nicholson, H., The magmatic evolution of Krafla, NE Iceland, Ph.D. thesis, University of Edinburgh, 1990.

Ochs, F. A., and R. A. Lange, The density of hydrous magmatic liquids, *Science*, *283*(5406), 1314–1317, 1999.

Ryan, M. P., Neutral buoyancy and the mechanical evolution of magmatic systems, in *Magmatic Processes: Physicochemical Principles*, edited by B. O. Mysen, pp. 259–287, Geochemical Society Special Publication 1, 1987b.

Ryan, M. P., Neutral buoyancy and the structure of mid-ocean ridge magma reservoirs, *Journal of Geophysical Research-Solid Earth*, *98*(B12), 22,321–22,338, 1993.

Sigurðsson, H., and R. S. J. Sparks, Lateral magma flow within rifted Icelandic crust, *Nature*, *274*, 126–130, 1978.

Slater, L., Melt generation beneath Iceland, Ph.D. thesis, University of Cambridge, 1996.

Sparks, R. S. J., and H. E. Huppert, Density changes during the fractional crystallization of basaltic magmas - Fluid dynamic implications, *Contributions to Mineralogy and Petrology*, *85*(3), 300–309, 1984.

Sparks, R. S. J., P. Meyer, and H. Sigurðsson, Density variation amongst mid-ocean ridge basalts - Implications for magma mixing and the scarcity of primitive lavas, *Earth and Planetary Science Letters*, *46*(3), 419–430, 1980.

Staples, R. K., R. S. White, B. Brandsdóttir, W. Menke, P. K. H. Maguire, and J. H. McBride, Faroe-Iceland Ridge Experiment. 1. Crustal structure of northeastern Iceland, *Journal of Geophysical Research-Solid Earth*, *102*(B4), 7849–7866, 1997.

Stolper, E., and D. Walker, Melt density and the average composition of basalt, *Contributions to Mineralogy and Petrology*, *74*(1), 7–12, 1980.

Walker, G. P. L., Viscosity Control of the Composition of Ocean Floor Volcanics, *Philosophical Transactions of the Royal Society, Series A*, *268*, 727–729, 1971.

Whittington, A., P. Richet, and F. Holtz, Water and the viscosity of depolymerized aluminosilicate melts, *Geochimica et Cosmochimica Acta*, *64*(21), 3725–3736, 2000.

Winpenny, B., and J. Maclennan, A partial record of mixing of mantle melts preserved in icelandic phenocrysts, *Journal of Petrology*, *52*(9), 1791–1812, 2011.

FIGURE CAPTIONS

Table 1. Parameters used in eruption modelling

Variable	Description	Dimensions
a	width of open fracture (dike)	m
h	magma chamber depth	km
G	shear modulus of country rock	Pa
ω	melt velocity	m s^{-1}
ρ	density	kg m^{-3}
μ	viscosity	Pa s
$\Delta\rho g$	buoyancy term	
P_f	overpressure required for fracture	Pa

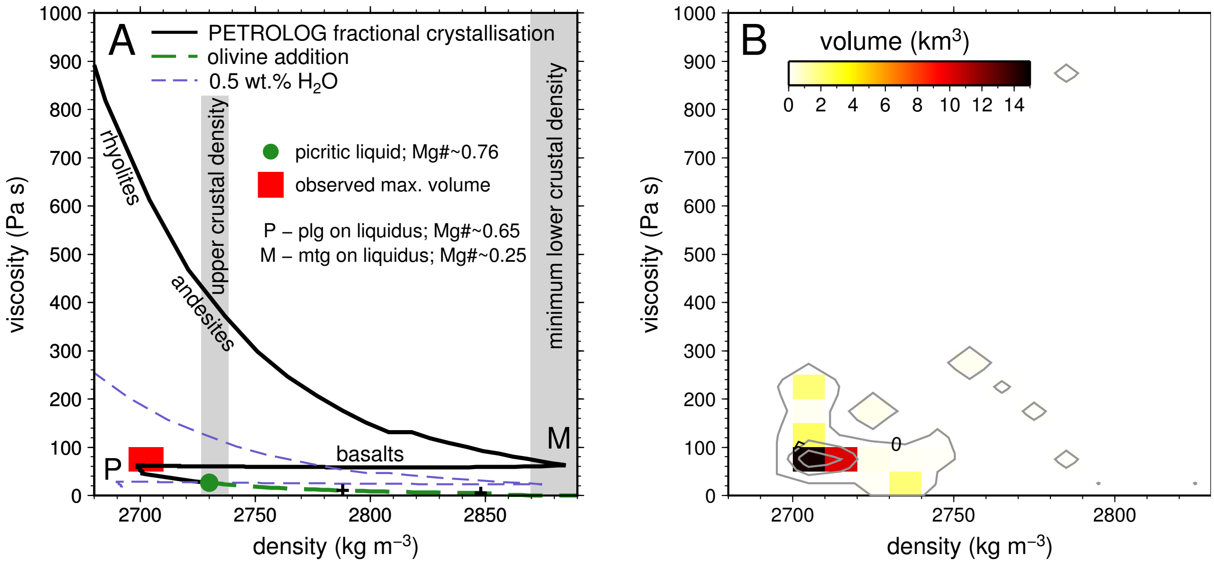

Figure 1. (A) Results of Petrolog3 fractional crystallisation model at 0.4 GPa. The initial composition, shown as a green circle, was a picrite from the NVZ whose whole-rock composition is in equilibrium with Fo_{92} olivine. The black solid line shows the density and viscosity of the melt during fractional crystallisation. The arrivals of plagioclase (plg) and magnetite (mgt) on the liquidus are associated with shifts in the density evolution of basalts. The thick green dashed line shows the effect of olivine accumulation in picritic melts; crosses indicate intervals of 10% olivine addition. The thin blue dashed line shows the effect of 0.5 wt.% H_2O on the density and viscosity of the liquid, calculated using the methods of *Ochs and Lange* (1999) and *Whittington et al.* (2000) respectively. (B) Relationship between erupted volume and estimated density and viscosity. The cumulative lava volume in each box was calculated and has been coloured according to the scale at the top and contoured in 5 km^3 intervals.

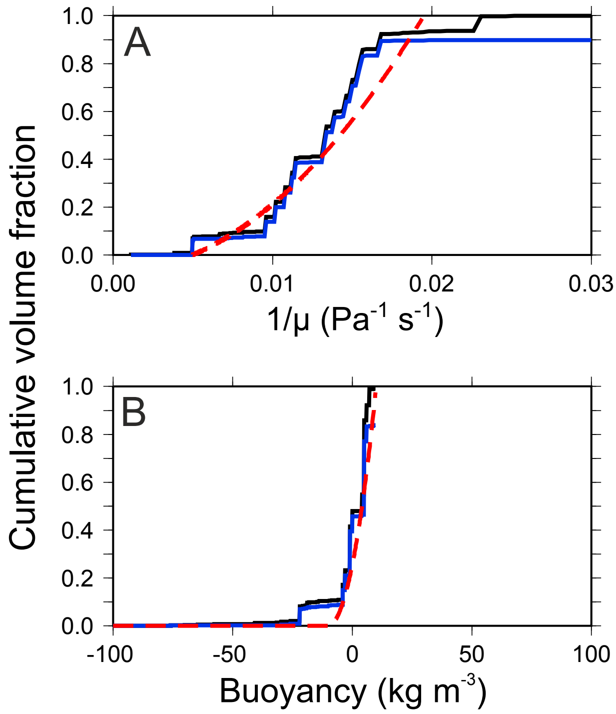

Figure 2. Comparison of sill model predictions and observed relationship between erupted volume and magmatic density and viscosity. (A) Cumulative histogram of the relationship between inverse viscosity and fraction of total erupted volume. All observations from the NVZ shown as a black continuous line. Samples with density under 2720 kg m^{-3} shown in blue. The predicted relationship between magma viscosity and maximum melt flux rate is shown as a dashed red curve. This curve was calculated only for magma with the viscosity range in samples with densities under 2720 kg m^{-3}. The density of the model magma was held constant at 2710 kg m^{-3} for these calculations. (B) Cumulative histogram showing the relationship between fractional erupted volume and density of samples relative to a reference density of 2710 kg m^{-3}. All samples shown as a black continuous line; those with viscosity under 100 Pa s shown as a blue line. The model results shown as a dashed red curve were calculated for the density range found in melts with viscosity under 100 Pa s. The viscosity of the model magma was held constant at 70 Pa s for these calculations.

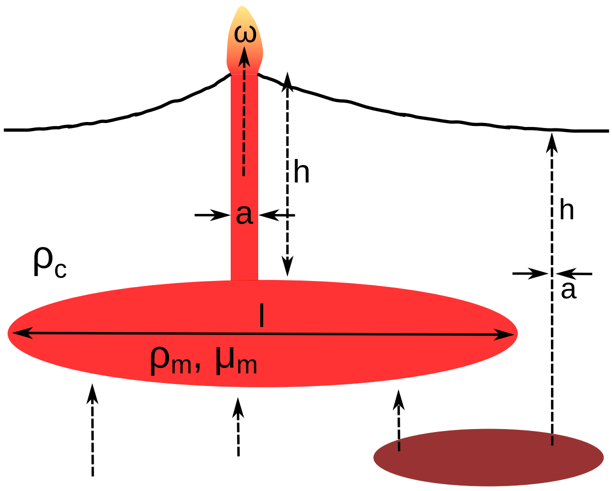

Figure 3. Schematic illustration of a crustal magma reservoir at depth h, with an open fracture allowing magma to ascend with velocity ω from the top of the reservoir. Modified after *Kelemen and Aharonov* (1998). The fracture of width a forms when the overpressure in the magma chamber exceeds the fracture stress of the crust. The magma reservoir may be fed directly by mantle melts or from deeper, sill-like melt lenses. Under certain conditions, high-density picritic magmas are enabled to erupt from deep magma chambers directly to the surface. See text for details.

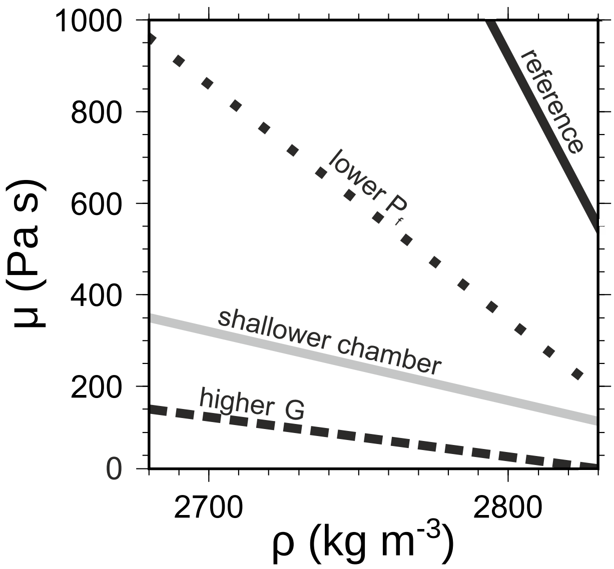

Figure 4. Results of constant volumetric influx rate models. Lines show boundary between density-viscosity corresponding to no predicted eruption (top right) and predicted eruption (bottom left). The solid black line shows an arbitrary reference set of conditions, with magma chamber depth at h=20 km, P_f=5 MPa and G=25 GPa. Note that eruption is expected for a wide range of magma densities and viscosities from this chamber. The other lines show the effect of varying the parameters individually, all in a sense which reduces the range of melt densities and viscosities that can be erupted. Dotted black line: effect of reducing P_f to 4 MPa, with all other parameters set at the reference values. Solid grey line: effect of setting h=10 km with all other parameters set at the reference values. Dashed black line: effect of increasing G to 50 GPa, with all other parameters set at the reference values.